

Numerical study on air cooling of Lithium-ion Battery pack

LuuKieu Oanh¹, Nguyen Minh Chau^{2*}

^{1,2}Faculty of Vehicle and Energy Engineering, Thai Nguyen University of Technology, Thai Nguyen, Vietnam

ABSTRACT:

Greenhouse gases (GHG) emissions are one of the major problems that the world is facing nowadays. The transportation sector, which relies mostly on internal combustion engines powered by fossil fuel oil, stands as one of the largest contributors to GHG emissions. The development of electric vehicles to meet the allowed GHG limits has recently been the main focus of research worldwide. Lithium-ion batteries are widely used as an energy source for electric vehicles. However, their batteries generate a lot of heat during the charging and discharging process. This heat can lead to a decrease in the efficiency of the battery and also the safety of the vehicle. Therefore, it is necessary to optimize the design of the battery cooling solution. In this study, the thermal behaviour of Lithium-ion battery pack is numerically investigated. The thermal management of the cells in the module is achieved based on forced air cooling. The computations of the temperature distribution in the module are performed with a three-dimensional modelling approach. The influences of discharge C-rate and inlet velocity quantity on the thermal behaviour of the battery pack are analyzed. The result indicated that the maximum temperature at discharge rates of 0.5C and 2 C are 301.215K and 309.319K, which present 0.41% and 3.11% of temperature rise, respectively. Furthermore, the maximum temperature reduces with the rise of the inlet velocity.

KEYWORDS: Cooling performance; Lithium-ion battery module; Air cooling strategies; ANSYS Fluent.

Date of Submission: 02-06-2023

Date of acceptance: 12-06-2023

I. INTRODUCTION

With the expansion of global demand for energy resources, particularly fossil fuels, people worldwide are facing threats such as environmental pollution, global warming, and energy crises. Fossil fuels, such as coal, oil, and natural gas, have served as the primary energy source worldwide for hundreds of years. Developed over millions of years from organic matter, these finite resources have fueled global economic progress over the past century. However, as the demand for fossil fuels continues to climb, their limited availability has caused a significant increase in prices. This issue is particularly pressing in the transportation sector, which is vital for global commerce and connectivity. Currently, the majority of transportation heavily relies on internal combustion engines that run on fossil fuel oil, as alternative energy sources for this purpose are still in the process of development [1,2]. Unfortunately, the use of fossil fuels poses a grave environmental concern due to the release of greenhouse gases (GHGs), contributing to global warming that impacts every corner of the globe [3,4]. Notably, the transportation sector stands out as one of the largest contributors to GHG emissions, responsible for approximately one-third of the total emissions in the U.S. [5]. To address the emission of greenhouse gases and reduce energy shortages, significant attention has been focused to green energy and clean vehicles.

Stephen et al. proposed the establishment of safety and testing standards through international and cross-industry collaborations to facilitate the development of clean vehicles [6]. Clean vehicles, including pure electric vehicles (EVs), hybrid electric vehicles (HEVs), plug-in hybrid electric vehicles (PHEVs), and fuel cell electric vehicles (FCEVs), offer effective solutions for reducing greenhouse gas and pollutant emissions while conserving energy when compared to conventional internal combustion vehicles (ICEVs) [7]. Li-ion batteries are considered the most suitable energy storage system in electric vehicles (EVs) due to several advantages, such as high energy and power density, long cycle life, and low self-discharge compared to the other rechargeable battery types. The thermal management of lithium-ion batteries plays a crucial role in their overall performance, including energy efficiency, cycling life, and discharge capacity. It is generally recommended to operate lithium-ion batteries within a temperature range of 20°C to 40°C for optimal performance [8]. Higher discharge rates in these batteries can lead to an increase in surface temperature. To decrease the rapid temperature rise and enhance the stability of lithium-ion batteries during discharge and charging processes, researchers have explored various battery thermal management systems (BTMS). These systems include strategies such as air cooling [9], liquid cooling [10], phase change materials (PCMs) [7], and heat pipes [11].

In this study, the thermal behaviour of Lithium-ion battery pack is numerically investigated. The thermal management of the cells in the module is achieved based on forced air cooling. The computations of the temperature distribution in the module are performed with a three-dimensional modelling approach. The influences of discharge C-rate and inlet velocity quantity on the thermal behavior of the battery pack are analyzed. The result indicated that the maximum temperature at discharge rates of 0.5C and 2 C are 301.215K and 309.319K, which present 0.41% and 3.11% of temperature rise, respectively. Furthermore, the maximum temperature reduces with the rise of the inlet velocity.

II. COMPUTATIONAL DOMAIN AND GOVERNING EQUATIONS

In the present study, the battery pack consists of several rows of 18650 batteries. Each row contains four batteries (as shown in Figure 1a). However, the computational domain is created, as shown in Figure 1b. The battery thermos-physical parameters are shown in Table 1 [12]. Along the flow direction, the cooling air just entering the battery pack conducts cooling air convection heat transfer on the battery surface, cooling the front module and heating the air itself; its cooling ability decreases, thus the temperature of the rear module will be higher than the front.

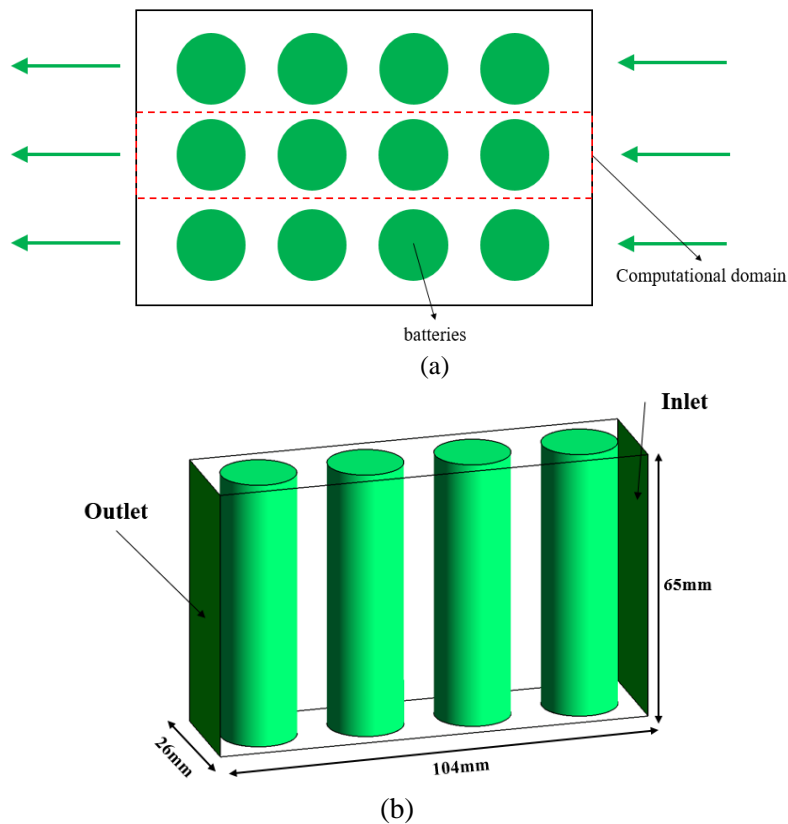


Figure 1. Schematic of battery pack (a) and computational domain (b)

Table 1. Physical and thermal properties of the 18650 li-ion battery.

Rated Voltage (V)	3.6	Specific Heat Capacity ($J.kg^{-1}K^{-1}$)	1200	Density ($kg.m^{-3}$)	2722
Length	65	Diameter (mm)	18	Anisotropic thermal conductivity ($W.m^{-1}K^{-1}$)	$k_x = 0.2$ $k_z = 37.6$

The computational domain is discretized using structured hexahedral mesh elements (Figure 2a). The grid is clustered near the wall vicinity of batteries in order to take into account the strong gradients in this region. The middle plane of the battery module, where it was used to take place results, is shown in Figure 2b.

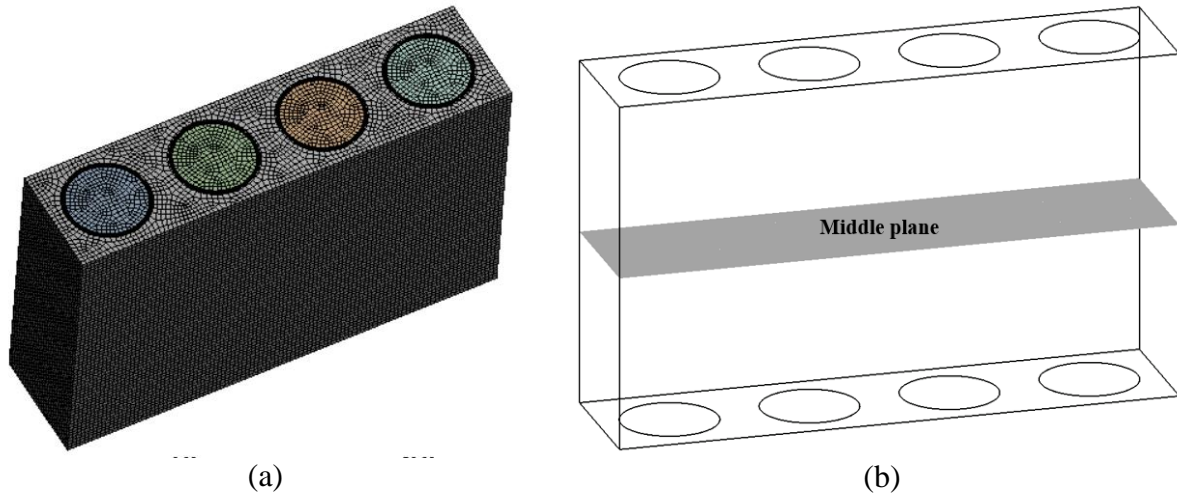


Figure 2. a) Close-up of mesh elements of battery pack; b) The middle plane of computational domain

In ANSYS-Fluent, the governing equations include the continuity, momentum, and energy equations. For the cooling air, these equations are shown as:

Continuity equation:

$$\frac{\partial \rho}{\partial t} + \nabla(\rho u) = 0 \quad (1)$$

Momentum equation:

$$\rho \frac{\partial u}{\partial t} + \rho u \cdot \nabla u = -\nabla p + \eta \nabla^2 u \quad (2)$$

Energy equation:

$$\frac{\partial(\rho c_p T)}{\partial t} + \nabla(\rho c_p u T) = \nabla(k \nabla T) \quad (3)$$

For the battery cell, the energy governing equation is expressed by:

$$\rho c_p \frac{\partial T}{\partial t} = \nabla(k \nabla T) + q \quad (4)$$

where ρ , c_p , T , p , k and q denote the density, specific heat, temperature, pressure, heat conductivity coefficient, the heat generation rate per unit volume of the battery, respectively.

A battery is considered as uniform a heat source. The heat generation rate per unit volume is expressed as equation 5.

$$q = a_0 + a_1 t + a_2 t^2 + \dots + a_n t^n \quad (5)$$

Where $a_0 \sim a_n$ are coefficients corresponding to the polynomial fitting method, q (W/m^3) is the heat generation rate and t (sec) is the time passed. These values were taken from [13]. The heat generation model is defined as an energy source term incorporated into CFD simulation using a user-defined function (UDF).

The standard k- ϵ model is selected which has been widely validated in modeling general low-speed and low-pressure flow around obstacles [14]. The k- ϵ turbulence model includes two equations for the turbulent kinetic energy k and the turbulent kinetic energy dissipation rate ϵ .

Turbulent kinetic energy equation:

$$\frac{\partial}{\partial t}(\rho k) + \frac{\partial}{\partial x_j}(\rho k u_j) = \frac{\partial}{\partial x_j} \left(\left(\mu + \frac{\mu t}{\alpha k} \right) \frac{\partial k}{\partial x_j} \right) + Gk + Gb - \rho \epsilon - YM + Sk \quad (6)$$

Turbulent kinetic energy dissipation equation:

$$\frac{\partial}{\partial t}(\rho \epsilon) + \frac{\partial}{\partial x_j}(\rho \epsilon u_j) = \frac{\partial}{\partial x_j} \left(\left(\mu + \frac{\mu t}{\alpha \epsilon} \right) \frac{\partial \epsilon}{\partial x_j} \right) + C1 \epsilon \frac{\epsilon}{k} (Gk + C3 \epsilon Gb) - \rho C2 \epsilon \frac{\epsilon^2}{k} + S\epsilon \quad (7)$$

where k and ϵ denote turbulent kinetic energy and turbulent dissipation rate, respectively.

The settings for the boundary conditions are as the following. The inlet and outlet are set as the velocity inlet and the pressure outlet, respectively. The top and bottom are defined as walls. Also, side one and side two are defined as the wall as well. In addition, the interfaces between batteries and fluid are defined as coupled walls.

The convergence criterion, i.e., the scaled residual, for both mass, momentum and energy equations are set to 10^{-5} and 10^{-6} , respectively, in each time step of the flow.

To analyze mesh independency, three mesh sizes are tested: 118.300, 236.405 and 475.500 elements. The mesh density was almost doubled in each refinement. The second one (236.405 elements) is used in the simulation (Fig. 2a)

The effects of time steps on the results are also tested using 50, 150 and 200 steps per cycle. Finally, 150 steps per cycle are used for the simulation in the transient regime.

IV. RESULTS AND DISCUSSION

The maximum temperature (T_{max}) and the maximum temperature difference (ΔT_{max}) are crucial parameters for evaluating the performance of a battery thermal management system (BTMS). ΔT_{max} represents the highest temperature difference observed between the batteries and it serves as a key indicator of the system's effectiveness in regulating and controlling battery temperatures.

Figure 3 shows the streamlines of battery module. Figure 3. (a) shows that the flow is smooth and the fluid resistance and the degree of turbulence are small in the small inlet velocity. Figure 3. (b) shows that the flow resistance and the turbulence degree are bigger, the heat transfer capacity of battery and cooling liquid flow will increase, which improves the cooling performance of the pack.

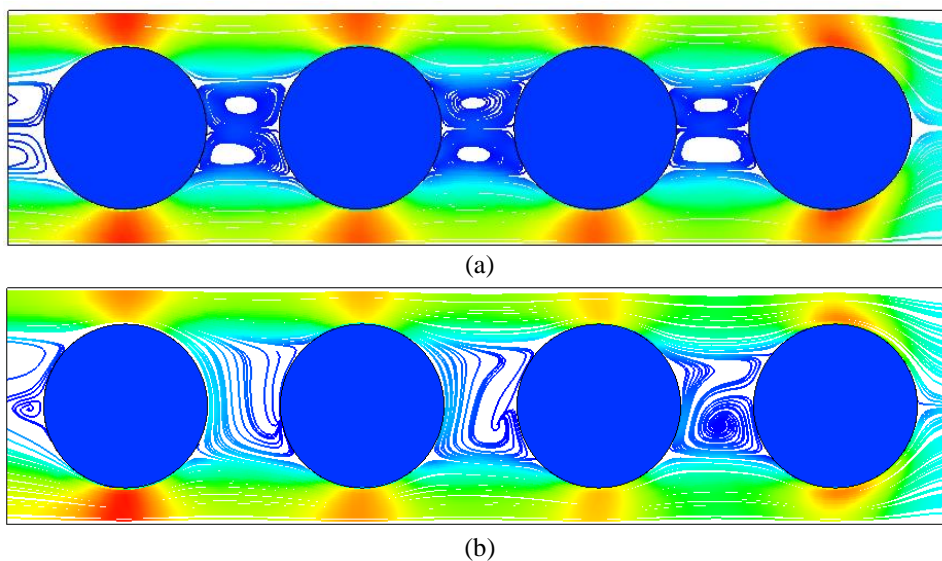
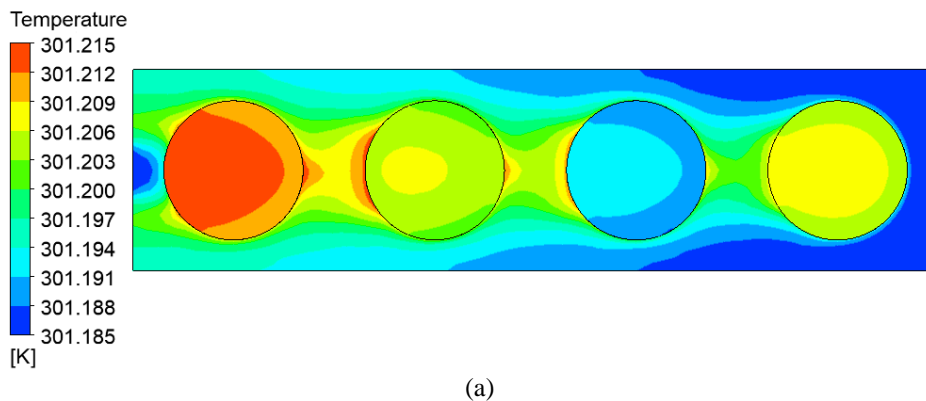
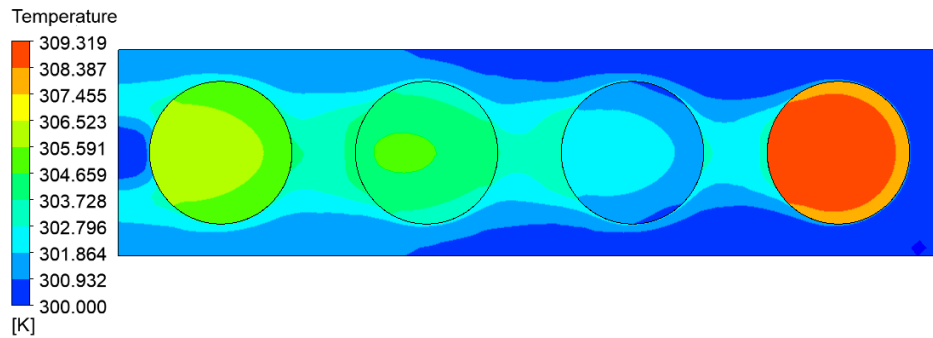


Figure 3. Streamlines of battery module at different inlet velocity: a) 1 ms^{-1} , b) 3 ms^{-1} .

The maximum temperatures of the battery pack of discharge for different C-rates are shown in Fig. 4. It is obvious that the maximum cell temperature during 0.5C and 2C are increased. The maximum temperature at discharge rates of 0.5C and 2 C are respectively 301.215K and 309.319K, which present 0.41% and 3.11% of temperature rise, respectively. By checking Fig. 4's temperature plots, it is concluded that the coolest battery is placed behind the first battery, while the battery with the maximum temperature is placed nearest or furthest from the inlet flow, depending on the discharge rate.



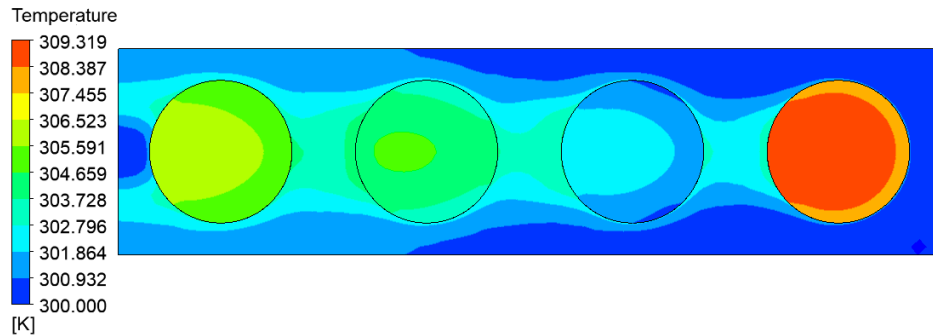
(a)



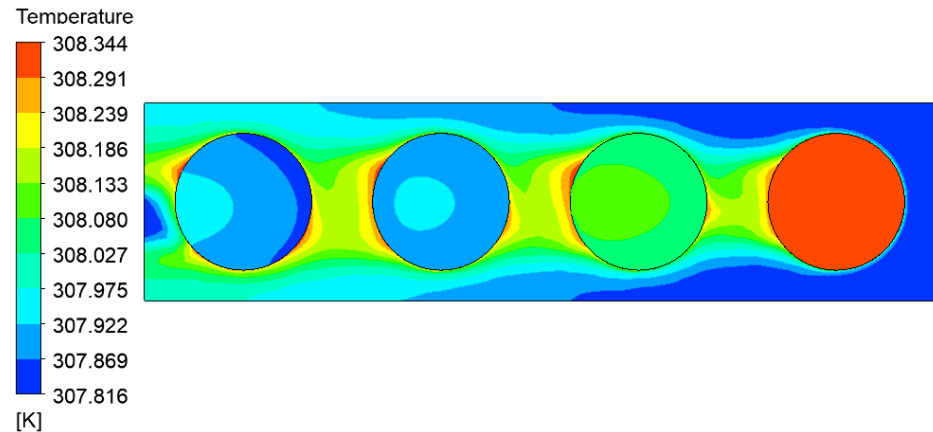
(b)

Figure 4. The evolution and distribution of temperature in battery pack through discharge under different C-rates (with same inlet velocity of 1 ms^{-1})

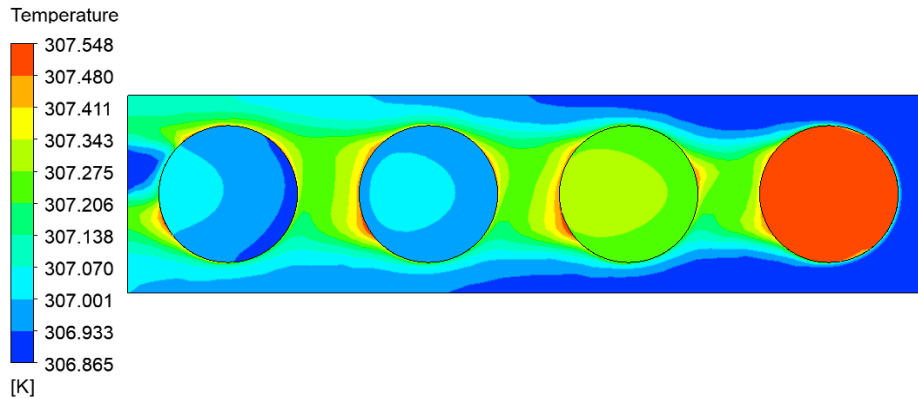
Figure 5 shows the temperature distribution of the middle section of the computational (see Figure 2) at different inlet air velocities at 2C discharge rates. The T_{max} reduces with the rise of the inlet velocity because the convective heat transfer coefficient on the battery surface increases. It is true that increasing the inlet velocity will raise the power consumption of the fan and then increase the operating load of the battery system. Therefore, when the air cooling system parameters are designed for a BTMS, an inlet velocity needs to be considered.



(a)



(b)



(c)

Figure 6. The temperature distribution of the middle section at different inlet velocities: a) 1 ms⁻¹ b) 2 ms⁻¹; c) 3 ms⁻¹.

Figure 6a demonstrates the T_{max} with different inlet velocity for discharge rate = 2C. Specifically, the T_{max} reduces with the rise of the inlet velocity. Figure 6b shows the variation of ΔT_{max} with different inlet velocity. It can be seen that the maximum temperature difference (ΔT_{max}) increases with increasing of the inlet velocity. Based on the previous analysis, it has been established that increasing the input speed results in improved cooling efficiency. However, the challenge lies in selecting an input speed that strikes a balance between high cooling efficiency and minimizing the temperature difference between the batteries.

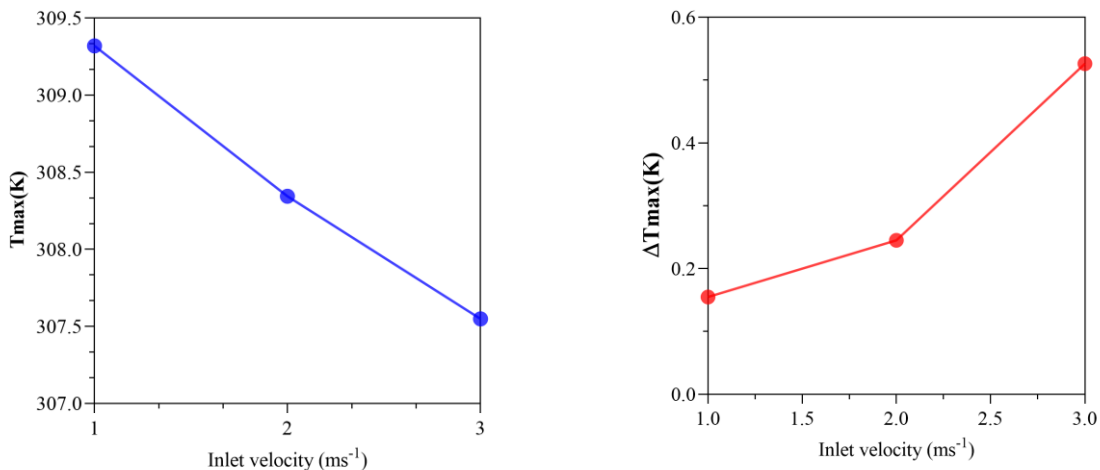


Figure 7. a) Variation of T_{max} with different inlet velocity, b) Variation of ΔT_{max} with different inlet velocity.

V. CONCLUSION

A numerical study on the influences of discharge C-rate and inlet velocity quantity on the thermal behavior of the battery pack was conducted. The thermal management of the battery pack is achieved based on a forced air cooling. The main conclusions of this work can be summarized as follows.

- At the same inlet velocity, the maximum temperature at discharge rates of 0.5C and 2 C are 301.215K and 309.319K, which present 0.41% and 3.11% of temperature rise, respectively.
- Increasing the inlet velocity results in a decrease in the maximum temperature of the cells.
- The temperature difference between the cells increases with an increase in inlet velocity.

Acknowledgment

The authors would like to express our gratitude to the Thai Nguyen University of Technology for support of this work.

REFERENCES

- [1]. Mata, T. M., Martins, A. A., and Caetano, Nidia. S., 2010, "Microalgae for Biodiesel Production and Other Applications: A Review," *Renewable and Sustainable Energy Reviews*, 14(1), pp. 217–232.
- [2]. Reitz, R. D., Ogawa, H., Payri, R., Fansler, T., Kokjohn, S., Moriyoshi, Y., Agarwal, A., Arcoumanis, D., Assanis, D., Bae, C., Boulouchos, K., Canakci, M., Curran, S., Denbratt, I., Gavaises, M., Guenther, M., Hasse, C., Huang, Z., Ishiyama, T., Johansson, B., Johnson, T., Kalghatgi, G., Koike, M., Kong, S., Leipertz, A., Miles, P., Novella, R., Onorati, A., Richter, M., Shuai, S., Siebers,

- D., Su, W., Trujillo, M., Uchida, N., Vaglieco, B. M., Wagner, R., and Zhao, H., 2020, "IJER Editorial: The Future of the Internal Combustion Engine," *International Journal of Engine Research*, 21(1), pp. 3–10.
- [3]. Hannon, M., Gimpel, J., Tran, M., Rasala, B., and Mayfield, S., 2010, "Biofuels from Algae: Challenges and Potential," *Biofuels*, 1(5), pp. 763–784.
- [4]. Bayro-Kaiser, V., and Nelson, N., 2017, "Microalgal Hydrogen Production: Prospects of an Essential Technology for a Clean and Sustainable Energy Economy," *Photosynth Res*, 133(1–3), pp. 49–62.
- [5]. United States Environmental Protection Agency, 2021, "Sources of Greenhouse Gas Emissions" [Online]. Available: <https://www.epa.gov/ghgemissions/sources-greenhouse-gas-emissions>. [Accessed: 26-Feb-2021].
- [6]. Brown, S., Pyke, D., and Steenhof, P., 2010, "Electric Vehicles: The Role and Importance of Standards in an Emerging Market," *Energy Policy*, 38(7), pp. 3797–3806.
- [7]. Rao, Z., and Wang, S., 2011, "A Review of Power Battery Thermal Energy Management," *Renewable and Sustainable Energy Reviews*, 15(9), pp. 4554–4571.
- [8]. Greco, A., Jiang, X., and Cao, D., 2015, "An Investigation of Lithium-Ion Battery Thermal Management Using Paraffin/Porous-Graphite-Matrix Composite," *Journal of Power Sources*, 278, pp. 50–68.
- [9]. Fan, L., Khodadadi, J. M., and Pesaran, A. A., 2013, "A Parametric Study on Thermal Management of an Air-Cooled Lithium-Ion Battery Module for Plug-in Hybrid Electric Vehicles," *Journal of Power Sources*, 238, pp. 301–312.
- [10]. Panchal, S., Khasow, R., Dincer, I., Agelin-Chaab, M., Fraser, R., and Fowler, M., 2017, "Thermal Design and Simulation of Mini-Channel Cold Plate for Water Cooled Large Sized Prismatic Lithium-Ion Battery," *Applied Thermal Engineering*, 122, pp. 80–90.
- [11]. Putra, N., Ariantara, B., and Pamungkas, R. A., 2016, "Experimental Investigation on Performance of Lithium-Ion Battery Thermal Management System Using Flat Plate Loop Heat Pipe for Electric Vehicle Application," *Applied Thermal Engineering*, 99, pp. 784–789.
- [12]. Behi, H., Karimi, D., Behi, M., Ghanbarpour, M., Jaguemont, J., Sokkeh, M. A., Gandoman, F. H., Berecibar, M., and Mierlo, J. V., 2020, "A New Concept of Thermal Management System in Li-Ion Battery Using Air Cooling and Heat Pipe for Electric Vehicles," *Applied Thermal Engineering*, 174, p. 115280.
- [13]. Hwang, F. S., Confrey, T., Scully, S., Callaghan, D., Nolan, C., Kent, N., and Flannery, B., 2020, "MODELLING OF HEAT GENERATION IN AN 18650 LITHIUM-ION BATTERY CELL UNDER VARYING DISCHARGE RATES," *Proceeding of 5th Thermal and Fluids Engineering Conference (TFEC)*, Begellhouse, New Orleans, LA, USA, pp. 333–341.
- [14]. Xing, J., Liu, Z., Huang, P., Feng, C., Zhou, Y., Zhang, D., and Wang, F., 2013, "Experimental and Numerical Study of the Dispersion of Carbon Dioxide Plume," *Journal of Hazardous Materials*, 256–257, pp. 40–48.